THE AMERICAN MINERALOGIST, VOL. 55, JANUARY-FEBRUARY, 1970

DELRIOITE AND METADELRIOITE FROM MONTROSE COUNTY, COLORADO[1]

MARIE LINDBERG SMITH, *U. S. Geological Survey, Washington, D. C. 20242.*

ABSTRACT

Single crystal X-ray studies of delrioite from the Jo Dandy mine, Montrose County, Colorado, show that two phases are intimately intergrown with parallel fiber axes. The relative intensities of the pattern of the two phases vary in response to changes in the humidity of the ambient atmosphere. Delrioite, the more hydrous of the phases, is monoclinic, with $a=17.170$, $b=7.081$, $c=14.644$ Å, $\beta=102°29'$; space group Ia or $I2/a$. Many of the delrioite crystals exhibit twinning with (100) the twin plane. The suggested unit-cell contents are 8 [$CaSrV_2O_6(OH)_2 \cdot 3H_2O$]. The calculated density is 3.16 g/cm^3. Metadelrioite, the less hydrated phase, is triclinic with $a=7.343$, $b=8.382$, $c=5.117$ Å, $\alpha=119°39'$, $\beta=90°16'$, $\gamma=102°49'$. Metadelrioite crystals are oriented with (001) parallel to (110) or ($1\bar{1}0$) of delrioite. Fiber axes a of metadelrioite and c of delrioite are parallel, $2a_M=c_D$. The suggested unit-cell contents of metadelrioite are 2 [$CaSrV_2O_6(OH)_2$]; the calculated density is 4.20 g/cm^3. A sample containing both delrioite and metadelrioite was dehydrated over P_2O_5; the analyzed dried fibers yielded 5.9 percent H_2O and had a measured specific gravity of 4.3. The difference in cell volume between delrioite and metadelrioite corresponds to an average volume of 25.17 Å^3 for each water molecule in delrioite.

INTRODUCTION

In 1959 Thompson and Sherwood described a new mineral, delrioite, from the Jo Dandy mine, Montrose County, Colorado. The formula $CaSrV_2O_6(OH)_2 \cdot 2H_2O$ was derived from the oxide ratios $CaO \cdot SrO \cdot V_2O_5 \cdot 3H_2O$,[2] on the assumption that the conditions of formation would more likely produce a metavanadate than a pyrovanadate.

The results of Thompson's preliminary examination by X-ray diffraction rotation and Weissenberg techniques indicate that the period of the fiber axis is "2 times 3.65 Å" and that fibers are both twinned and "rotated with respect to each other about their mutual axis of elongation" (Thompson and Sherwood, 1959). A re-examination of Thompson's X-ray diffraction patterns shows evidence for two phases. A new set of diffraction patterns by Weissenberg and precession camera techniques establish one of the phases as monoclinic, here designated as delrioite, and the other phase as triclinic, here designated as metadelrioite. The pattern of the monoclinic phase disappears when the fibers are exposed to a dry atmosphere and reappears when the dried fibers are exposed to a humid atmosphere. The presence of the patterns of two phases in the X-ray patterns taken by Thompson at the time of the original study

[1] Publication authorized by the Director, U. S. Geological Survey.

[2] The ratio $H_2O:CaO$, recalculated from Sherwood's chemical analyses, table 3, is 3.5:1, not 3:1 as originally reported.

suggests that the material selected for chemical analysis also contains both phases.

The description and name, metadelrioite, were approved in advance of publication by the Commission on New Minerals and Mineral Names, IMA.

Delrioite

Delrioite and metadelrioite are intergrown with parallel fiber axes. Specimens of crystal intergrowths prepared for X-ray study may be dehydrated over P_2O_5 until the X ray pattern of delrioite disappears. Upon exposure of the dried fibers to an atmosphere saturated with water vapor, the delrioite pattern reappears. The mixed phases may also be dehydrated to a single phase by heating at temperatures of 90°–100°C and rehydrated by exposure to a humid atmosphere. The intensity of the pattern of each phase increases or decreases in proportion to the amount of that phase present at a given point in the hydration or dehydration process (Figure 1). In patterns from intergrowths that have been subjected to repeated cycles of hydration and dehydration, the peak heights gradually diminish and reflections are broadened, with concomitant loss of resolution of individual reflections.

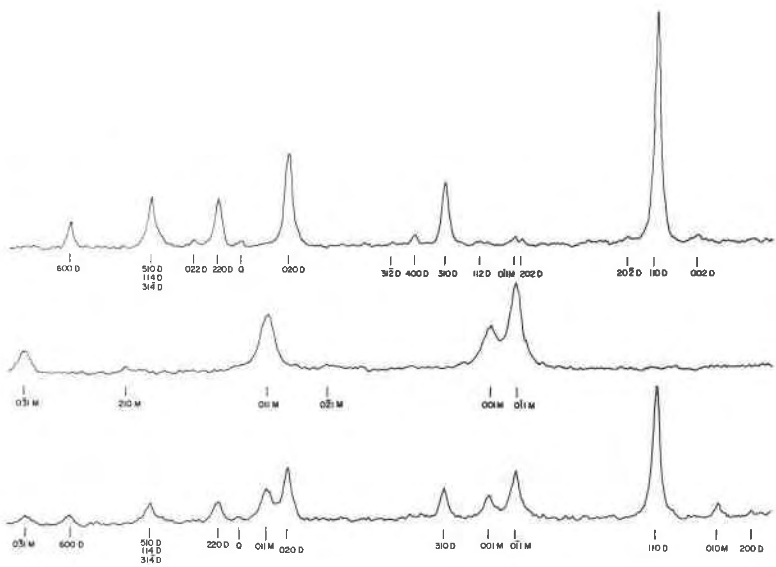

Fig. 1. Diffractometer patterns of delrioite and metadelrioite. The lower pattern represents the original pattern of the mixed phases, with delrioite reflections indicated as *D* and metadelrioite reflections as *M*; Q=quartz. The middle pattern represents the same diffractometer mount after exposure to a dry atmosphere and the upper pattern represents the rehydration of the dried material. Note change of peak heights, relative to the original pattern, upon hydration and dehydration.

The Weissenberg and Buerger precession photographs of delrioite intergrown with metadelrioite show systematic variations in certain classes of reflections allotted to delrioite. These variations are accounted for by considering that some of the delrioite crystals (photographed in three dimensions) are not twinned but other delrioite crystals are twinned with (100) the twin plane. The symmetry of delrioite was derived from the nontwinned crystals. Delrioite (Table 1) is monoclinic, with a large true cell, space group *Ia* or *I2/a*. Only the reflections corresponding to a smaller pseudocell with space group *C*2, *Cm*, or *C2/m* are strong enough to be represented in the powder diffraction pattern (Fig. 1). An alternate pseudocell, space group $B2_1/d$, with $\beta = 90°10'$ may be obtained from the true cell by the transformation $2 0\frac{1}{2}/010/00\frac{1}{2}$. The *c* common to both pseudocells is the fiber axis "2×3.65 Å" identified by Thompson in the initial study (Thompson and Sherwood, 1959). Measurements from the single-crystal studies were applied in the refinement of the powder diffractometer data by Appleman and Appleman using the least-squares method of Evans, Appleman, and Handwerker (1963). The unit-cell data for delrioite are given in Table 1; the calculated and measured interplanar spacings are given in Table 2.

In Figure 2, the *h*1*l* Buerger precession pattern from a nontwinned crystal of delrioite is spliced with one from a twin to show the arrangement of reflections along row lines. The interpretation of the patterns is illustrated by the accompanying grid. In the pattern of the nontwinned crystal reflections along any *h*1*l* row line, *l* constant, are separated by steps of 2 in *h*. In the patterns of the twinned crystal, extra reflections are observed on row lines $l \neq 4n$. On row lines $l = 4n$, reflections from original crystal and from twinned counterpart superimpose owing to the near equality of $a^* = 0.0597$ Å^{-1} and $4c^* \cos \beta^* = 0.0605$ Å^{-1}. On other lattice levels—*h*0*l*, *l* constant; *hk*2, *k* constant, and *hk*4, *k* constant, reflections along row lines are separated by steps of 2 in *h* in the nontwinned crystals, but on these levels the pattern of metadelrioite is superimposed ($h0l_D$ and $hk0_M$; $hk2_D$ and $1kl_M$; $hk4_D$ and $2kl_M$). In the patterns of the twin crystal additional reflections are observed on *hk*2 row lines, *k* constant.

The patterns of both delrioite and metadelrioite have been identified in Thompson's "single crystal" Weissenberg photographs. The material selected by Thompson and Sherwood (1959) for chemical analysis is assumed to contain the same two phases as identified in Thompson's X-ray diffraction photographs. Oxide ratios (Table 3, column 3) have been recalculated from the analysis of Sherwood. From these ratios the average composition of $CaSrV_2O_6(OH)_2 \cdot 2\frac{1}{2}H_2O$ is obtained for the partially dehydrated mixture. This mixture has a measured specific gravity of 3.1 ± 0.1.

TABLE 1. CRYSTALLOGRAPHIC DATA FOR DELRIOITE AND FOR METADELRIOITE (PRESENT STUDY)

Delrioite (monoclinic)			Metadelrioite (triclinic)
Choice of space groups			
True cell	Pseudocell	Pseudocell	$P\bar{1}$ or $P1$
Ia or $I2a$	$C2$ or Cm or $C2/m$	$B2_1/d$	
Unit-cell constants[a]			
$a=17.170\pm0.003$ Å	17.170 Å	33.53 Å	$a=7.343\pm0.007$ Å
$b=$ 7.081 0.001	7.081	7.081	$b=8.382$ 0.003
$c=14.644$ 0.004	7.322	7.322	$c=5.117$ 0.004
			$\alpha=111°39'\pm0°02'$
$\beta=102°29'\pm0°01'$	102°29′	90°10′	$\beta=$ 90°16′ 0°05′
			$\gamma=102°49'$ 0°04′
Volume 1738 Å^3	869 Å^3	1738 Å^3	283.5 Å^3
			$a^*=0.1403\pm0.0001$ Å^{-1}
			$b^*=0.1325$ 0.0001
			$c^*=0.2112$ 0.0002
			$\alpha^*=67°42'\pm0°02'$
			$\beta^*=84°31'$ 0°04′
			$\gamma^*=76°04'$ 0°04′
			Volume* 0.003527 Å^{-3}
Probable unit cell contents: $8[CaSrV_2O_6(OH)_2 \cdot 3H_2O]$			$2[CaSrV_2O_6(OH)_2]$
Calculated density	3.16 g/cm^{-3}		4.21 g/cm^3
Measured specific gravity			4.3

[a] Least squares refinement of the diffractometer powder data of delrioite, artificially hydrated, and of metadelrioite artificially dehydrated, each to a single phase; $\lambda=1.5418$ Å; temperature 75°F. In the naturally occurring intergrowths, a of metadelrioite is exactly equal $\frac{1}{2}c$ of delrioite ($=7.32$ Å) in rotation and in Buerger precession patterns, V-filtered Cr radiation $\lambda=2.2909$ Å, and Ni-filtered Cu radiation, $\lambda=1.5418$ Å.

Insufficient material is available to provide a chemical analysis of the fully hydrated sample. The water of hydration should exceed $2\frac{1}{2}$ molecules in the formula unit $CaSrV_2O_6(OH)_2 \cdot nH_2O$. The waters of hydration are lost upon conversion to metadelrioite. The amount of water that may be added to a constant volume of 217 Å^3 occupied by one formula unit in delrioite is limited in that the molecular weight of the end product of hydration is fixed by the measured specific gravity of the mixture. If

TABLE 2. X-RAY POWDER DIFFRACTION DATA FOR DELRIOITE AND FOR METADELRIOITE

Previous study[a]		Mixed phases[b]		Present study									
				Delrioite[c]					Metadelrioite[d]				
				Calculated		Measured			Calculated		Measured		
						Single crystal	X-ray powder diffractometer data				Single crystal	X-ray powder diffractometer data	
I	*d*(Å)	*I*	*d*(Å)	*hkl*	*d*(Å)	*I*[5]	*I*	*d*(Å)	*hkl*	*d*(Å)	*I*[e]	*I*	*d*(Å)
				200	8.382	vw	vw	8.385*					
									010	7.546	vw		
w	7.2	25	7.15	002	7.149	ms	vw	7.132*	100	7.127	nr		
s	6.5	100	6.52	110	6.523	s	vs	6.525*					
f	6.2	8	6.12	$\bar{2}02$	6.133	ms	vw	6.121*					
		6	5.93						$\bar{1}10$	5.944	mw		
				$\bar{1}12$	5.034	vw							
ms	4.95	83	4.928	202	4.938	m	vw	4.936*	$0\bar{1}1$	4.942	ms	s	4.944*
w	4.74	6	4.725						001	4.734	m	ms	4.732*
									110	4.652	m	w	4.651*
		6	4.647										
				112	4.629	w							
m	4.40	46	4.389	310	4.387	m	ms	4.387*					
		5Q	4.251										
		4	4.174	400	4.191	w	w	4.191*	$1\bar{1}1$	4.175	w	vw	4.167*
		2	4.141						$\bar{1}01$	4.130	vw	vw	4.125*
				$\bar{3}12$	4.058	mw							
				$\bar{4}02$	4.014	w							
		5	3.965						$\bar{1}\bar{1}1$	3.955	w		
									101	3.781	a		
									020	3.773	w	w	3.778*
									$\bar{1}20$	3.726	mw	vw	3.732*
		4	3.713						$0\bar{2}1$	3.717	vw		
				$\bar{2}04$	3.579	ms							
		9	3.582	004	3.574	ms			$\bar{2}10$	3.571	vw		
									200	3.564	vw		
m	3.55	25	3.535	020	3.540	s	s	3.539*	$1\bar{2}1$	3.539	w		
				312	3.485	mw							
ms	3.45	60	3.452						011	3.462	ms	s	3.457*
f	3.35	19Q	3.343	402	3.316								
									$\bar{1}11$	3.362	a		
w	3.27	16	3.257	220	3.261	mw	ms	3.261*					
				$\bar{1}14$	3.252	a							
f	3.18	12	3.175	022	3.173	mw	vw	3.171*					
									$\bar{1}\bar{2}1$	3.096	w		
		5	3.062	$\bar{4}04$	3.066	ms	vw	3.063	120	3.045	w		
				$\bar{2}22$	3.066								
				204	3.058	ms							
				$\bar{3}14$	3.034	mw		3.035*					
				510	3.030	m		3.031*					
				114	3.029	mw		3.028*					
				$\bar{5}12$	3.009	w							
									$\bar{2}01$	2.988	mw	vw	2.984*
									$2\bar{1}1$	2.973	w		
									$\bar{2}20$	2.972	s	w	2.973*
									210	2.959	s	w	2.958*
									111	2.915	w	vw	2.920*
				222	2.877	vw							
				$\bar{6}02$	2.817	vw			$\bar{2}\bar{1}1$	2.814	mw }	vw	2.810
									$2\bar{2}1$	2.810	mw }		

TABLE 2—(*Continued*)

Previous study[a]		Mixed phases[b]		Present study									
				Delrioite[c]					Metadelrioite[d]				
				Calculated		Measured			Calculated		Measured		
						Single crystal	X-ray powder diffractometer data				Single crystal	X-ray powder diffractometer data	
I	d(Å)	I	d(Å)	hkl	d(Å)	I^5	I	d(Å)	hkl	d(Å)	I^e	I	d(Å)
mw	2.80	16	2.797	600	2.794	ms	ms	2.794*				vw	2.797
									$\bar{2}11$	2.743	w	vw	2.747*
									201	2.725	w		
				420	2.705	a			$1\bar{3}1$	2.697	vw	w	2.704
w	2.69	21	2.685						$0\bar{3}1$	2.682	m	ms	2.683*
				$\bar{4}22$		vw							
				512	2.613	w	vw	2.610*					
w	2.57	25	2.571	$\bar{5}14$	2.573	ms	w	2.572*	130	2.574	w	w	2.571*
				314	2.566	ms	w	2.567*					
									$\bar{1}21$	2.553	vw	w	2.558
									$0\bar{1}2$	2.552	mw	m	2.547
									021	2.521	a		
w	2.51	12	2.515	$\bar{2}24$	2.517	mw	vw	2.516	030	2.515	m	m	2.516*
				024	2.515	mw	vvw	2.512					
		7	2.474	$\bar{6}04$	2.476	mw							
				404	2.469	mw			$0\bar{2}2$	2.471	a		
		5	2.430	$\bar{2}06$	2.435	m	vw	2.436	$\bar{3}10$	2.440	w		
				602	2.430	vw							
				422	2.420	a			$\bar{1}\bar{1}2$	2.419	w		
									$2\bar{3}1$	2.388	vw		
		4	2.386 (Broad)	006	2.383	mw	vw	2.384*					
									$\bar{2}\bar{2}1$	2.387	vw		
									$1\bar{1}2$	2.386	w		
									$1\bar{2}2$	2.378	vw }		
									300	2.376	mw }		2.379
									002	2.368	w	mw	2.370
									$\bar{1}31$	2.358	vw		2.364
									$\bar{2}30$	2.337	vw		
				130	2.337	vw		2.337					
				031	2.329	mw	w	2.330	220	2.326	vw	vw	2.326
		7	2.317	$\bar{4}24$	2.318	w		2.324					
				224	2.314	w		2.316	$\bar{1}02$	2.314		vw	2.316
				$\bar{7}12$	2.303	vw			$\bar{2}21$	2.300	a	vw	2.305
				$\bar{1}16$	2.301	a			$\bar{1}\bar{2}2$	2.294	w		
				$\bar{4}06$	2.296	w			211	2.286			
				710	2.269	w			$\bar{3}20$	2.272	w		
				$\bar{3}16$	2.261	vw							
				$\bar{1}32$	2.242		vw	2.242*	121	2.233	w	w	2.237*
									130	2.211	w		
									$\bar{3}01$	2.211	vw		
									$3\bar{1}1$	2.191	vw		
				$\bar{6}22$	2.204	vw							
				132	2.202		vw	2.202					
				620	2 193	vw	vw	2.194*	$0\bar{3}2$	2.187	a		
									102	2.185			
				116	2.180	vw		2.177					

(*Continued on next page*)

Table 2—(*continued*)

Previous study[a]		Mixed phases[b]		Present study									
				Delrioite[c]					Metadelrioite[d]				
				Calculated		Measured			Calculated		Measured		
						Single crystal	X-ray powder diffractometer data				Single crystal	X-ray powder diffractometer data	
I	*d*(Å)	*I*	*d*(Å)	*hkl*	*d*(Å)	*I*[5]	*I*	*d*(Å)	*hkl*	*d*(Å)	*I*[e]	*I*	*d*(Å)
mw	2.18	10	2.174	330	2.174	mw	m	2.174*					
				206	2.172	vw		2.170					
				$\bar{8}02$	2.140	mw							
				$\bar{3}32$	2 131		vw	2.132*					
f	2.12	7	2.121	$\bar{7}14$	2.122		vw	2.122*					
				512	2.117		vw	2.120					
				800	2.096	m	w	2.096	$1\bar{4}1$	2.084		vw	2.084*
		5	2.016	$\bar{6}24$	2.029			2.026	$\bar{1}\bar{3}2$	2.023		vw	2.013
				424	2.025			2.022					
				$\bar{1}34$	1.984				$\bar{1}32$	1.984			
		6	1.980	026	1.977				$\bar{3}30$	1.980	mw		
				316	1.960			1.960	$\bar{3}21$	1.945	a		
									$\bar{1}40$	1.943	w	w	1.945
f	1.93	5	1.932						031	1.938	mw	w	1.938*
												w	1.931
w	1.89	10	1.886						040	1.886	s	m	1.885*
									$1\bar{4}2$	1.874		w	1.874*
f	1.85	5	1.855						$0\bar{4}2$	1.858	mw	m	1.859*
									230	1.855	m	w	1.855
									$\bar{1}41$	1.855	a		
		16	1.830										
m	1.80	10	1.803										
		7	1.789										
		8	1.766										
		5	1.661										
		11	1.626										

[a] Thompson and Sherwood (1959); Cu K_α, $\lambda = 1.5418$ Å, camera diameter 114.59 mm.; measurements not corrected for film shrinkage. Cut-off 15 Å. s = strong, m = medium, w = weak, f = faint.

[b] Powder pattern, naturally occurring mixed crystals, V-filtered Cr radiation, $CrK\alpha_{ave.}$, $\lambda = 2.2909$ Å; camera diameter 114.59 mm. Averaged *d*-spacings films 15080 and 15089 of spindle 15076, each film corrected for film shrinkage; lower limit of 2θ measureable is 8°.

[c] Delrioite, artificially hydrated. Starred (*) interplanar spacings were used in the least-squares refinement of the powder diffraction data by Daniel E. Appleman and Margaret H. Appleman, see Table 1. Includes all possible calculated *d*-spacings >2.1 Å with $h+k=2n$, and $l=2n$, plus 031; other reflections permitted by the space groups $I2/a$ are too weak to suspect their presence in the diffractometer pattern. Diffractometer patterns, average of three, Ni-filtered Cu radiation, $K\alpha_{ave.}$, $\lambda = 1.5418$ Å; intensities estimated, *hk*0 intensities enhanced. Symbols vs = very strong, s = strong, ms = medium strong, m = medium, mw = medium weak, w = weak, vw = very weak, nr = not resolved (100 of metadelrioite and 002 of delrioite); *Q* reflection from quartz.

[d] Metadelrioite, artificially dehydrated. Includes all possible *d*-spacings >2.3 Å. Diffractometer patterns, average of three, Ni-filtered Cu radiation, $CuK\alpha_{ave.}$, $\lambda = 1.5418$ Å; intensities enhanced in the 0*kl* zone.

[e] Intensities estimated visually from precession and Weissenberg photographs of natural intergrowths of delrioite metadelrioite; patterns of different exposure times and radiations. Intensities obtained for partial listing only; a = absent, pattern available, but reflection too weak to be observed.

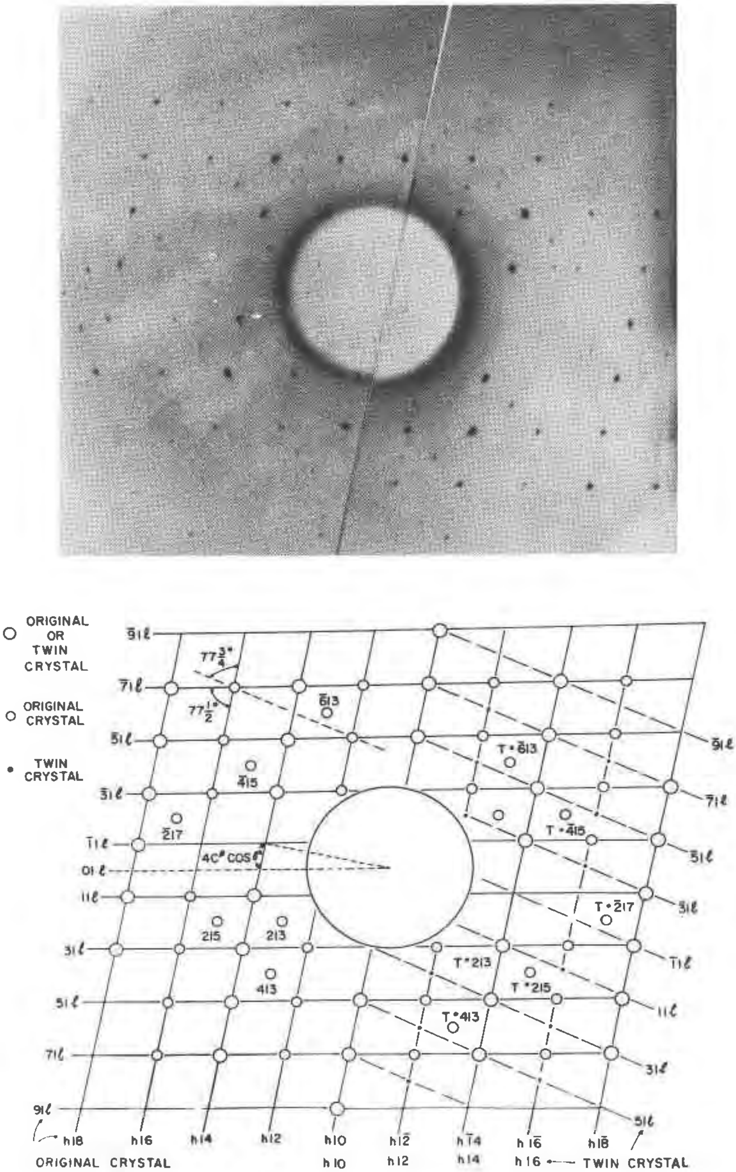

FIG. 2. Composite picture showing the $h1l$ pattern of a nontwinned crystal of delrioite (left) and of a twinned crystal (right); pattern spliced with $h10$ center row line left of splice. Reflections on lattice levels $l=4n$ are not resolved in original crystal and twinned counterpart (large circles). On lattice levels $l \neq 4n$ reflections in the original crystal and in the twinned counterpart are indicated by small circles and dots, respectively. Note especially the disposition of reflections repeated by twinning on row lines with l odd.

TABLE 3. CHEMICAL ANALYSIS AND CALCULATED COMPOSITION OF DELRIOITE AND OF METADELRIOITE

	Previous data[a]		New calculations				
	Analysis (wt %)	Analysis recalculated to 100 percent	Oxide[b] ratios	Delrioite[c] theoretical composition	Metadelrioite[d] theoretical composition	Analysis[e] recalculated to 100 percent with 5.9% H_2O	Theoretical[f] composition 5:1 mixture delrioite metadelrioite
CaO	13.30	13.5	1.00	13.56	15.60	14.9	13.86
SrO	24.50	24.8	0.99	25.05	28.82	27.5	25.60
V_2O_5	46.00	46.6	1.06	43.97	50.58	51.7	44.96
H_2O^+	5.64	5.7	1.31	17.42	5.00	5.9	15.58
H_2O^-	9.24	9.4	2.17				
SiO_2	1.30						
Total	99.98	100.0		100.00	100.00	100.00	100.00
Specific gravity							
Meas.	3.1±0.1					4.3	
Calc.				3.16	4.2		

[a] Chemical analysis by Alexander Sherwood in Thompson and Sherwood, 1959.

[b] Oxide ratios derived from chemical analysis by Sherwood recalculated on basis CaO=1; ratio total H_2O:CaO=3.48:1.

[c] Theoretical composition of $CaSrV_2O_6(OH)_2\cdot 3H_2O$.

[d] Theoretical composition of $CaSrV_2O_6(OH)_2$.

[e] Delrioite sample dehydrated in a desiccator over P_2O_5 contains 5.9% H_2O and has a measured specific gravity of 4.3 (Robert Meyrowitz, written communication). Sample gives X-ray pattern of metadelrioite. Analysis by Sherwood recalculated to 100% with water content of dehydrated phase (5.9%).

[f] The calculated composition of delrioite and metadelrioite in the sample analyzed by Sherwood approximates a mixture of $5[CaSrV_2O_6(OH)_2\cdot 3H_2O]+1[CaSrV_2O_6(OH)_2]$.

there are X molecules of delrioite with n H_2O and Y molecules of metadelrioite with $O\cdot H_2O$, then the total water of hydration in the bulk analyzed sample is given by $nX/(X+Y)=2.5$. For $n=3$, $X=5$ and $Y=1$; for $n=4$, $X=5$ and $Y=3$, etc. For $n=3$, delrioite has a calculated specific gravity of 3.16 and that of the mixture is 3.28. For $n=4$, delrioite has a calculated specific gravity of 3.51 and that of the mixture is 3.70. The value $n=3$ gives calculated specific gravities slightly higher than measured ones, but calculated specific gravities are unnecessarily high if $n>3$. Moreover, for $n=3$, the apparent average volume per water molecule involved in the delrioite-metadelrioite transformation is 25.17 Å^3 (calculated later in the paper). Comparable data for rossite-metarossite and for hewettite-metahewettite indicate that the apparent volume per water molecule involved in these transformations is about 25 Å^3 (Ahmed and Barnes, 1963; Barnes and Qurashi, 1952). The unit cell contents proposed for delriorite based upon the above considerations are $CaSrV_2O_6(OH)_2 \cdot 3H_2O$, $Z=8$. The calculated composition of delrioite is given in Table 3.

Metadelrioite

Naturally occurring intergrowths of delrioite and of metadelrioite have parallel fiber axes: *c* of delrioite and *a* of metadelrioite, with $\frac{1}{2}c_D \cong a_M$. In this orientation, the *hk*0 net of delrioite and the 0*kl* net of metadelrioite are superimposed (Figure 3). Moreover, the 00*l* row line of metadelrioite coincides with the *hh*0 row line of delrioite. The intergrowths are thus oriented such that (001) of triclinic metadelrioite is parallel to (110) of monoclinic delrioite. If the dehydration of delrioite and the concomitant growth of metadelrioite is initiated at different points in delrioite, possibly only a few unit cells apart, then metadelrioite crystals may be formed with equal probability as right crystals $(001)_M \| (110)_D$ or as left crystals $(001)_M \| (1\bar{1}0)_D$, using first letter symbols for the two minerals. As dehydration progresses the crystals grow towards each other and eventually coalesce. The oriented intergrowths thus will have the general appearance of twinned crystals.

Direct cell relationships between the two phases are illustrated in Figure 4, projection down *c* of delrioite. The interfacial angles, $(010)_D \wedge (110)_D \| (001)_M$ is 22°54′, and $(001)_M \wedge (05\bar{8})_M$ is 23°05′ making $(010)_D$ almost parallel $(05\bar{8})_M$. Then $(010)_D \wedge (010)_M = 90°36'(22°54' + \alpha_M^*)$ and $c \sin \beta_M$ makes an angle of 0°36′ with $[010]_D$. The angular divergence of $c \sin \beta_M$ and $-c \sin\beta_M$ with $[010]_D$ is less than the arcs through which the individual crystal planes reflect in the plane normal to the fiber axis (Figure 3); thus $hk0_M$ and $hk1_M$ (Fig. 5) from right and left crystals may be obtained by photographing these nets normal to $[010]_D$.

In Figure 5, the $hk1_M$ Buerger precession patterns of metadelrioite are spliced to show two upper level nets (left side of pattern) and four upper level nets (right side of pattern). The $0k1_M$ row line is common to Figure 3. The interpretation of the patterns, given by the grid, may be expressed:

$$
\begin{array}{ccccc}
M_{right} \xleftarrow[a_M \| c_D]{(001)_M \| (110)_D} & \nwarrow & & \nearrow & \xrightarrow[c_{\bar{D}} \| a_{\bar{M}}]{(110)_{\bar{D}} \| (001)_{\bar{M}}} \bar{M}_{right} \\
 & & D \xleftrightarrow[\text{twin relation}_D]{(100)_D \| (100)_{\bar{D}}} \bar{D} & & \\
M_{left} \xleftarrow[a_M \| c_D]{(001)_M \| (1\bar{1}0)_D} & \nearrow & & \nwarrow & \xrightarrow[c_{\bar{D}} \| a_{\bar{M}}]{(1\bar{1}0)_{\bar{D}} \| (001)_{\bar{M}}} \bar{M}_{left}
\end{array}
$$

2 lattices M (left pair)

4 lattices M (all)

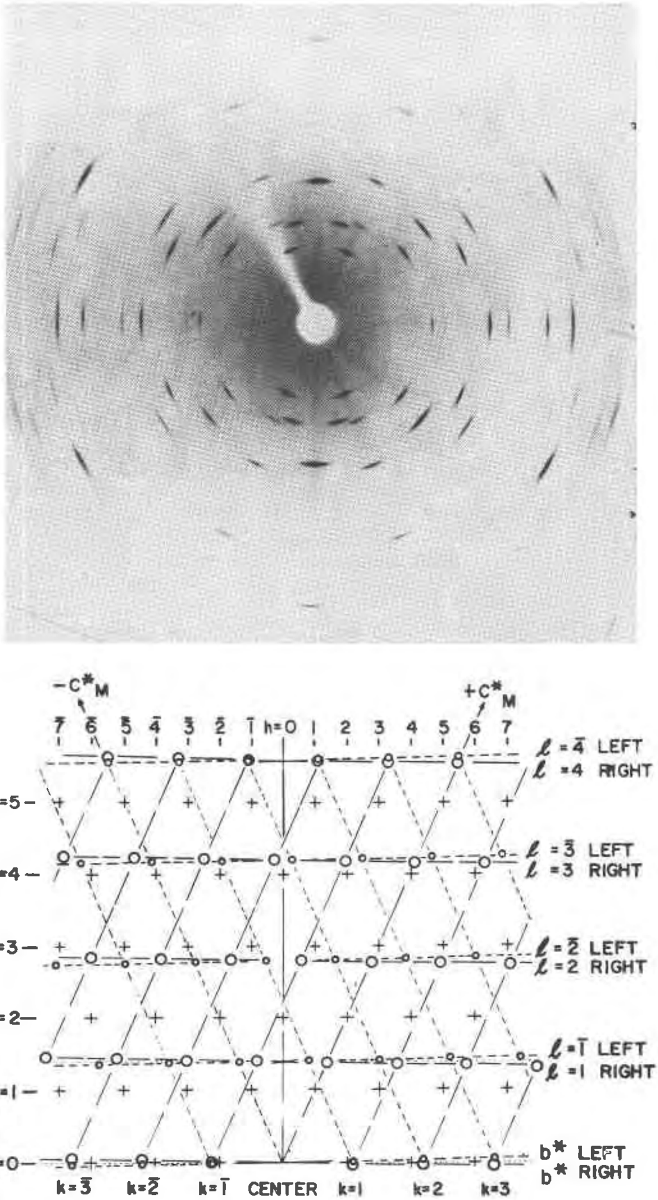

FIG. 3. Superposition of 0*kl* of metadelrioite on *hk*0 of delrioite. Row line *h*10 of delrioite common with Fig. 2, *h*1*l*; row lines 0k1 and 0k$\bar{1}$ of metadelrioite common with Fig. 5, *hk*1. Possible reflections delrioite indicated by +; grid for *k* at left and *h* at top. Possible reflections right metadelrioite crystal large circles on dashed lines, row line $00l_M$ parallel $hh0_D$. Possible reflections left metadelrioite crystal small circles on short dashed lines, row line $00l_M$ parallel $hh0_D$. Grid for metadelrioite *k* at bottom and for *l* at right.

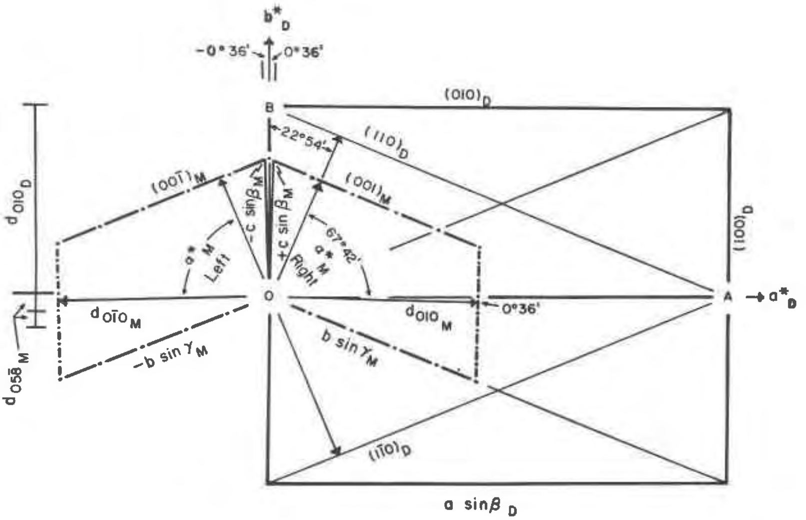

FIG. 4. Direct lattice, projection normal to fiber axes, *c* in delrioite and *a* in metadelrioite; delrioite solid lines, metadelrioite dashed lines.

On the left side of the pattern, note the order of descending *d* for reflections from right and left crystals, respectively, and the disposition of the four forms of 2$\bar{1}$1, 21$\bar{1}$, 2$\bar{1}\bar{1}$, and 211 from 2 lattices. On the right side of the figure, additional reflections, indicating the presence of 4 lattices, are resolved on row lines with *h* odd. For row lines with *h* even, reflections which indicate 4 lattices are not resolved from erflections indicating 2 lattices, due to the close approximation of $\frac{1}{2}b^*$ (0.0660 $Å^{-1}$) to 2a* cos γ^* (0.0677 $Å^{-1}$); *i.e.* 21$\bar{1}$ is not resolved from 2$\bar{2}$1, nor is 2$\bar{1}\bar{1}$ resolved from 201. The intensity distribution and disposition of all reflections on the *hk*0 (17 different integer metadelrioite reflections), *hk*1 (20), *h*0*l* (16) Buerger precession patterns, and 0*kl* (18), 1*kl* (23) and 2*kl* (28) Weissenberg patterns are accounted for by the superposition of the lattices given above.

The data from the single-crystal patterns were applied to the refinement of the unit-cell parameters from the diffractometer powder data for artificially dehydrated metadelrioite, by Daniel E. Appleman and Margaret H. Appleman, Tables 1 and 2.

Metadelrioite dried in a desiccator over P_2O_5 until the X-ray pattern of delrioite has disappeared contains 5.9 percent H_2O and has a measured specific gravity of 4.3 (Robert Meyrowitz, written communication). The analysis of Sherwood, recalculated to 100 percent but with 5.9 percent H_2O is compared with the calculated composition and density of $2[CaSrV_2O_6(OH)_2]$ in Table 3 (cell volume 283.5 $Å^3$). The latter formula

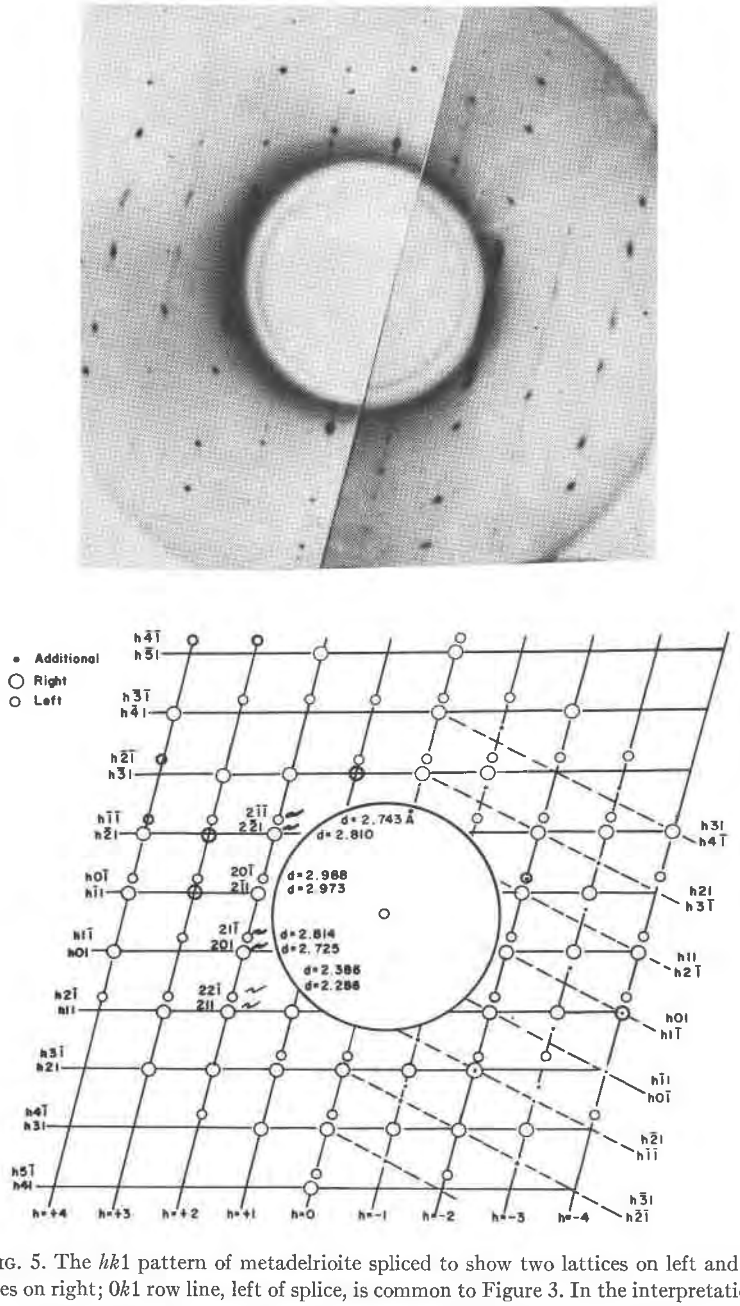

FIG. 5. The $hk1$ pattern of metadelrioite spliced to show two lattices on left and four lattices on right; $0k1$ row line, left of splice, is common to Figure 3. In the interpretation of the pattern note order of descending d alternates in pairs, $d_{21\bar{1}} > d_{2\bar{2}1}$ but $d_{2\bar{1}\bar{1}} > d_{201}$. Large circles represent right M_R crystal and small circles left M_L crystal, 2 lattices; additional reflections indicated by dot on row lines $h=1$ and $h=3$ from $\overline{M}$ crystals. On row lines $h=2$ and $h=4$ reflections corresponding to two (M_{R+L}) and four ($M_{R+L}+\overline{M}_{R+L}$) lattices are not resolved.

unit approximates the ratios derived from the recalculated analysis, but contains a whole number of cations and anions. It is herein proposed that the unit-cell contents of metadelrioite correspond to $CaSrV_2O_6(OH)_2$, $Z=2$, and the excess water (0.9 percent) in the dried fibers represents water not completely removed from the sample during the dehydration.

Relationships of Delrioite, Metadelrioite, and Other Vanadates

The derived unit-cell contents of delrioite are:

$$8[CaSrV_2O_6(OH)_2 \cdot 3H_2O];$$

the derived unit-cell contents of metadelrioite are:

$$2[CaSrV_2O_6(OH)_2].$$

The original analysis approximates a 5:1 (formula units) mixture of delrioite and of metadelrioite, Table 3.

Delrioite is formed under conditions which would more likely produce a metavanadate than a pyrovanadate (Evans in Thompson and Sherwood, 1959). The presence of rossite, $CaV_2O_6 \cdot 4H_2O$ and of metarossite $CaV_2O_6 \cdot 2H_2O$ at the same locality was noted by Thompson and Sherwood. Both rossite and metarossite were observed in the same hand specimen as delrioite and metadelrioite in the present study.

From the unit-cell volumes for rossite, $2(CaV_2O_6 \cdot 4H_2O)$ (Kelsey and Barnes, 1960) and for metarossite, $2(CaV_2O_6 \cdot 2H_2O)$ (Ahmed and Barnes, 1963), Ahmed and Barnes calculate an apparent volume per water molecule of 25.05 Å^3. Using this volume we may calculate that the apparent ionic volume occupied by nonwater oxygen is 18.7_4Å^3 both in rossite and in metarossite.

From the unit-cell volumes for delrioite, 1738 Å^3, and for metadelrioite, 283.5 Å^3, an apparent volume per water molecule of 25.17 Å^3 (1738 Å^3-$4\times$283.5 Å^3)/24 is obtained. The apparent average volume of the remaining O+OH in delrioite and in metadelrioite is 17.72 Å^3 (283.5 Å^3/16). The calculated average ionic volume occupied by oxygen and hydroxyl in delrioite and in metadelrioite is smaller than corrseponding volumes in rossite and in metarossite, calculated above, but is larger than the 17.4 Å^3 reported for häggite (Evans and Mrose, 1960) and the 17.2 Å^3 reported for montroseite (Evans and Block, 1953).

The chain length of the vanadium-oxygen coordinated polyhedra, represented by the fiber-axis sublength, 3.66 Å, is the same in naturally occurring delrioite and metadelrioite. In the artificially hydrated delrioite the chain length is 3.66 Å, and in the artificially dehydrated metadelrioite it is 3.67 Å. Every crystal intergrowth gives pseudo-orthorhombic diffraction patterns with regard to reflections on row lines or lattice levels with inter-row or interplanar spacings $\cong$3.66 Å. These lengths approximate the chain lengths 3.697 Å in $KVO_3 \cdot H_2O$ (Christ, Clark, and Evans, 1954) and 3.69 in $Sr(VO_3)_2 \cdot 4H_2O$ (Sedlacek and Dornberger-Schiff, 1965). They are slightly larger than the V—V separations across corner-shared oxygen atoms in rossite (3.51 and 3.56 Å, Ahmed and Barnes, 1963) and in metarossite (3.55 and 3.58 Å, Kelsey and Barnes, 1960). In each of these structures the fivefold oxygen-coordinated vanadium atoms form double chains of trigonal dipyramids. The vanadium atoms in each chain corner-share oxygen atoms. Each corner-shared oxygen atom in one chain is also on or near the equatorial plane with the vanadium atom in the other chain. The two chains are linked together in a zigzag pattern by oxygen atoms sharing edges of the trigonal dipyramids. The pseudocell dimensions ($B2_1/d$ setting) of delrioite are such that the arrangement of the oxygen-coordinated vanadium chains may be only slightly modified in detail from their arrangement in $Sr(VO_3)_2 \cdot 4H_2O$. In $Sr(VO_3)_2 \cdot 4H_2O$, space group $C112_1/d$, $a=7.38$, $b=33.6$, $c=7.16$ Å, $\beta=90°$ [should be γ] (Sedlacek and Dornberger-Schiff, 1965).

The calcium and strontium coordination of these structures is quite different. In rossite and in metarossite (Ahmed and Barnes, 1963; Kelsey and Barnes, 1960) the calcium is surrounded by eight $O+H_2O$ in roughly cubic coordination. In $Sr(VO_3)_2 \cdot 4H_2O$ the strontium atoms are surrounded by nine $O+H_2O$, six at the corners of a squat trigonal prism and three on the equatorial plane with the strontium atom. Only half the available strontium-oxygen polyhedra are occupied. Delrioite contains both kinds of atoms, calcium and strontium. The cross-linkage of calcium and strontium to each other and to vanadium is based upon a different number of oxygen-coordinated cation polyhedra in delrioite ($Ca+Sr:V=2:2$) from rossite ($Ca:V=1:2$) and from $Sr(VO_3)_2 \cdot 4H_2O$ ($Sr:V=1:2$) but the same number as in $KVO_3 \cdot H_2O$ ($K:V=1:1$). The modification in structural detail required by the addition of both calcium and strontium between the double chains of oxygen coordinated vanadium atoms is not known.

The hydration to delrioite and the dehydration to metadelrioite is accomplished by exposures of the intergrowth to extreme conditions of wetness and dryness. The proportion of metadelrioite reflections to delrioite reflections in successive X-ray patterns from the same natural intergrowth does not appear to vary with small changes in room temperature and humidity.

Acknowledgments

The author wishes to thank Mary E. Thompson for making her mineral specimens and her partially studied X-ray rotation and Weissenberg patterns of delrioite available for the present study. Robert Meyrowitz, of the U. S. Geological Survey, determined the specific gravity and water content of a sample artificially dehydrated to metadelrioite. Daniel E. Appleman and Margaret H. Appleman, of the U. S. Geological Survey, refined the unit-cell parameters of artificially hydrated delrioite and artificially dehydrated metadelrioite from the powder diffractometer data. Mary E. Mrose, also of the U. S. Geological Survey, originally examined a portion of the type delrioite sample for Mary E. Thompson, and she noted the presence of patterns of two phases.

References

Ahmed, F. R., and W. H. Barnes (1963) The crystal structure of rossite. *Can. Mineral.* **7**, 713–726.

Barnes, W. H., and M. M. Qurashi (1952) Unit cell and space group data for certain vanadium minerals. *Amer. Mineral.* **37**, 407–422.

Christ, C. L., J. R. Clark, and H. T. Evans, Jr. (1954) The crystal structure of potassium metavanadate monohydrate, $KVO_3 \cdot H_2O$. *Acta Crystallogr.* **7**, 801–807.

Evans, H. T. Jr., D. E. Appleman, and D. S. Handwerker (1963) The least squares refinement of crystal unit cells with powder diffraction data by an automatic computer indexing method. *Amer. Crystallogr. Ass. Meet., Cambridge, Mass., Prog. Abstr.*, p. 42.

Evans, H. T. Jr., and S. Block (1953) The crystal structure of montroseite, a vanadium member of the diaspore group. *Amer. Mineral.* **38**, 1242–1250.

Evans, H. T. Jr., and M. E. Mrose (1960) Crystal chemical study of the vanadium oxide minerals, häggite and doloresite. *Amer. Mineral.* **45**, 1144–1166.

Kelsey, C. H., and W. H. Barnes, (1960) The crystal structure of metarossite. *Can. Mineral.* **6**, 448–466.

Sedlacek, P., and K. Dornberger-Schiff (1965) Das Strukturprinzip des Strontium-metavanadat, $Sr(VO_3)_2 \cdot 4H_2O$: *Acta Crystallogr.* **18**, 407–410.

Thompson, M. E., and A. M. Sherwood (1959) Delrioite, a new calcium strontium vanadate from Colorado. *Amer. Mineral.* **44**, 261–264.

Manuscript received, August 21, 1969; accepted for publication September 29, 1969.